Journal of Nuclear Materials 393 (2009) 108–113

Contents lists available at ScienceDirect

Journal of Nuclear Materials

journal homepage: www.elsevier.com/locate/jnucmat

Spark Plasma Sintering of simulated radioisotope materials within tungsten cermets

R.C. O'Brien [a,*], R.M. Ambrosi [a], N.P. Bannister [a], S.D. Howe [b], H.V. Atkinson [c]

[a] University of Leicester Space Research Centre, University Road, Leicester LE1 7RH, UK
[b] Center for Space Nuclear Research, Idaho National Laboratory, ID 83415-3855, USA
[c] University of Leicester, Department of Engineering, University Road, Leicester LE1 7RH, UK

ARTICLE INFO

Article history:
Received 24 February 2009
Accepted 18 May 2009

PACS:
07.77.−n
07.87.+V
25.85.Ca
28.90.+i
28.41.Bm
28.41.Kw
28.50.Hw
28.50.Ky

ABSTRACT

A Spark Plasma Sintering (SPS) furnace was used to produce ceramic–metallic sinters (cermets) containing a simulated loading of radioisotope materials. CeO_2 was used to simulate loadings of PuO_2, UO_2 or AmO_2 within tungsten-based cermets due to the similar kinetic properties of these materials, in particular the respective melting points and Gibbs free energies. The work presented demonstrates the capability and suitability of the SPS process for the production of radioisotope encapsulates for nuclear fuels and other applications (including waste disposal and radioisotope power and heat source fabrication) where the mechanical capture of radioisotope materials is required.

1. Introduction and overview of the Spark Plasma Sintering technique

The encapsulation of radioisotope materials such as $^{238}PuO_2$ and $^{241}AmO_2$ within tungsten cermets is of particular interest for the production of radioisotope heat sources for thermal management and radioisotope power systems [1]. The production of nuclear fuels for fission reactor systems based upon W–UO_2 or W–UN cermets is also of particular interest for increased operational safety and security. It has previously been proposed that plutonium dioxide or americium dioxide could be encapsulated within a tungsten-based cermet using the Spark Plasma Sintering (SPS) technique [1]. The fundamental rationale for carrying out SPS processing trials for these materials was that traditional sintering techniques (such as hot isostatic pressing or 'HIPping') required the materials to be processed at temperatures that were high enough to exceed the dissociation temperatures of the radioisotope oxides. The result would then be the formation of complete or partial non-cermet regions such as those described in the fuel element development summary in the General Electric report on the development of the 710 High-Temperature Gas Reactor [2]. SPS is capable of processing materials at greatly reduced temperatures and processing times [3], while minimising the grain growth typically attributed to traditional techniques [4]. Grain growth is highly detrimental to the process of densification during sintering. It has been demonstrated in partially densified samples of urania produced by hot pressing that a larger number of pores occur on the faces of grains that have undergone grain growth and hence have a reduction in grain boundary contact area, whereas smaller grains which have not undergone grain growth have pores concentrated at the grain corners [5]. The pores located in between the faces of grain boundaries have a greater degree of mobility than those pinned at the corners of grain boundaries [6] and hence in extreme cases the grain boundaries break away from the pores resulting in the encompassing of the pores within the grains [7]. In such instances, the densification process is effectively halted [7], thus it is most ideal to minimise grain growth during sintering in order to maximise the effectiveness of the densification process. In addition, large grains give rise to a reduction in overall material strength and hence grain growth should be avoided. For these reasons, SPS is highly suited to the production of high density cermets with temperature sensitive ceramics such as UO_2, PuO_2 and AmO_2.

In the SPS process, a powder mixture is heated by Joule heating which results from passing an electric current through the powder matrix requiring consolidation. This is effectively the same as conventional resistive heating with the exception that the temperature is varied during the process by the current pulse modulation. There are therefore two distinct operating temperatures for an SPS furnace; the average temperature, and a much higher temperature that is only reached during the flow of the current pulses. The

* Corresponding author. Tel.: +44 1162522902; fax: +44 1162522464.
E-mail address: rco3@star.le.ac.uk (R.C. O'Brien).

0022-3115/$ - see front matter © 2009 Elsevier B.V. All rights reserved.
doi:10.1016/j.jnucmat.2009.05.012

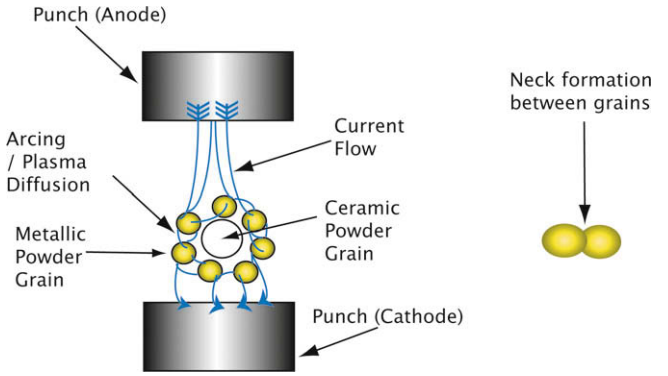

Fig. 1. The principal of Spark Plasma Sintering (SPS). (Left) Illustration of the effect of the application of a current pulse to the powdered materials between the two electrode punches. Current discharge causes arcing between conductive grains resulting in rapid localised heating which in turn results in the formation and diffusion of plasma between the conductive grains. (Right) As the current pulse is terminated, the diffused plasma cools resulting in the formation of necks between the material grains.

average temperature is tuned to be lower than the melting point of the materials in the matrix. This therefore reduces or prevents the dissociation of the ceramic materials that are to be encapsulated within the cermet.

During each current discharge, metallic material is transported as a plasma by the propagation of sparks across the pores of the matrix (see Fig. 1 Left). When the current is switched off, the matrix undergoes rapid cooling resulting in the condensation of the metallic vapours within the regions where there is mechanical contact between powder grains [8]. This condensation of vapour produces necks that consolidate these joints (See Fig. 1 Right). The material transport in subsequent spark pulses increases due to the greater electric current density in the necks and contacts than inside the body of each powder grain. The rate of material transport is enhanced by the application of an external compressive force [9] resulting in the plastic deformation of the powder grains at each interface [4] resulting in a flatter joint with lower electrical resistance. This process propagates throughout the matrix and is enhanced by the external pressure which induces the plastic flow of material to form a sintered cermet with a density that is very close the full theoretical density. This process of propagation is similar to that exhibited in the consolidation of matrices by hot isostatic pressing [4].

The overall SPS setup consists of a conductive (graphite) die into which the powder mixture is formed, a press and a high power pulsed DC circuit (see Fig. 2). The filled cavity in the die is capped on the top and bottom with graphite punches that are free to move in the axial direction, facilitated by the use of a suitable high temperature lubricant, such as grafoil, to lubricate the side walls of the die (see Fig. 3a). The die, punches and, ultimately, the

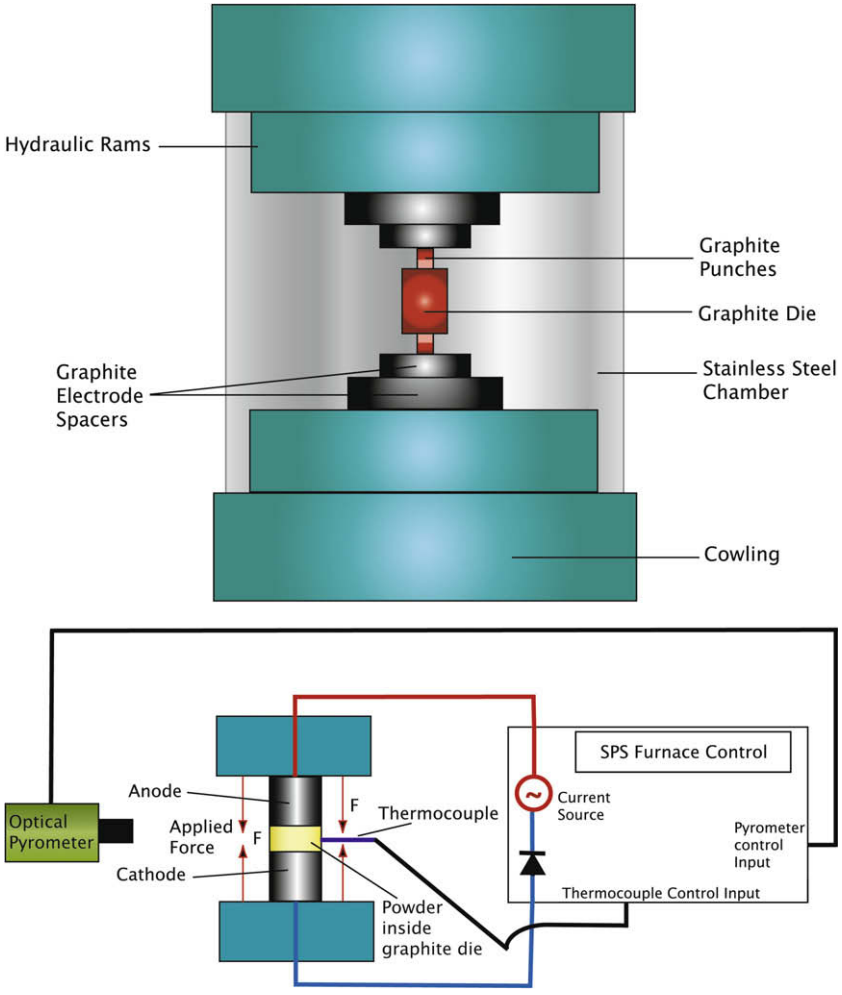

Fig. 2. (TOP) Schematic of the Spark Plasma Sintering furnace chamber containing an assembled graphite die and punches (manufactured by the user). (BOTTOM) Electrical schematic of the SPS furnace with associated temperature control electronics.

powder mixture itself, form the completing components for the DC circuit (see Fig. 2 Bottom). The geometry of the die determines the radial geometry of the pressed and sintered cermet. The ceramic powder (CeO_2) and tungsten metal powders are mixed to the specified volumetric ratio prior to loading into the graphite die. The die is then put under compression in between two electrodes in a hydraulic press [10] in order to compact the mixture. At this point a several kA current is passed through the material. The current pulse duration is of the order of several microseconds [8].

2. Experimental trials

The production of tungsten-based cermets loaded with radioisotope stimulants was carried out by fabricating CeO_2–W cermets. CeO_2 was selected as a simulant for radioisotope materials such as PuO_2, AmO_2 and UO_2 since ceria has very similar kinetic properties to these three compounds, in particular the respective melting points and Gibbs free energies.

Preliminary measurements were made of the densities of tungsten-only SPS sinters produced with two different tungsten powder grain sizes. It was found that the maximum density of sinters made from tungsten powder with an average grain size of 10 μm was 82.7% of the theoretical density of tungsten. For screened tungsten powder with a grain size of 3–6 μm, the maximum sinter density measured was 93.6% of the theoretical density of tungsten. The preliminary experimental tests also revealed that these densities could be achieved from a hold time of 20 min at a maximum temperature of 1500 °C. It should therefore be noted that the sintering process can be achieved at 44% of the melting temperature of tungsten (tungsten m.p. is approximately 3400 °C).

The CeO_2 feedstock used in the tungsten–ceria cermet fabrication had an average grain size of 75 μm. The 3–6 μm tungsten particle size was selected in order to ensure that a high cermet theoretical density could be achieved. Since the tungsten used in these cermets was designed to encapsulate the ceria, the larger CeO_2 powder size allowed the smaller grains of tungsten to fill

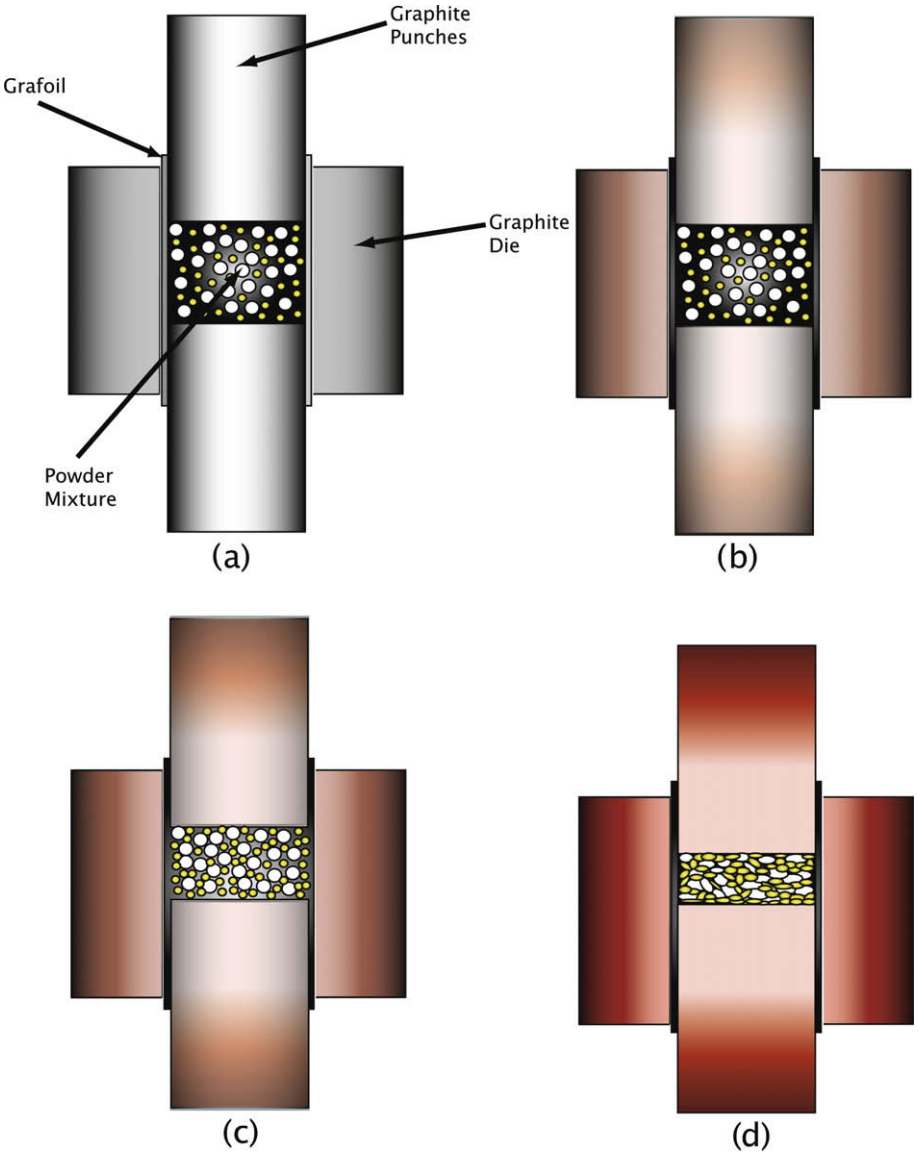

Fig. 3. (a) Punches and die assembly lined with grafoil containing mixed CeO_2 and tungsten powder. (b) The assembled die upon loading into SPS furnace (see Fig. 2 TOP). Application of minimal pressure and initiation of heating results in small expansion of the materials. (c) Application of pressure to the punches via the hydraulic rams of the SPS furnace facilitates initial densification by closing of voids. (d) Neck formation and continued application of pressure achieves final densification of the bulk materials resulting in cermet production.

the voids between the grains of CeO_2. Two mixture ratios of tungsten to ceria were used in these experiments for comparison. These ratios were 50% W to 50% CeO_2 and 60% W to 40% CeO_2 by volume. The dies used throughout this experimentation produced hexagonal sintered cermets with a side length of 11.7 mm and a footprint area of 3.543×10^{-4} m^2. Each die was loaded with 14 g of mixture, although gram quantities of material was frequently lost via leakage through the gaps in between the die and punches during the application of pressure after the assembled die was loaded into the SPS furnace. Minimisation of leakage within the furnace chamber was achieved by pre-pressing the filled die within a small hydraulic press.

Temperature control of the furnace is performed by an automatic programmable system that uses a signal input from either a thermocouple or an optical pyrometer. The calibrated range of operation for the furnace thermocouple is between 0 °C and 1200 °C. For this reason, temperature measurement during the production of tungsten-based cermets was performed using the optical pyrometer. The optical pyrometer had a calibration range between 570 °C and 2500 °C. In order to achieve repeatability in the production of the cermets, the automatic furnace controller was programmed to drive the temperature up to 600 °C by limiting the output current of the furnace driver such that 600 °C could not be exceeded during the ramp period. The values assigned to the output limits were derived through preliminary testing of the die and material compositions prior to the production trials presented within Section 3 of this paper. Once a temperature of 600 °C was achieved, the output limits were removed and control was then governed by the signal from the optical pyrometer. The result of this method of temperature control was in the form of a stepped sintering profile as illustrated in Fig. 4.

A hold time of 10 min is shown at 800 °C in the sintering profile. At the beginning of the 10 min hold, the pressure applied to the sample was increased from 12.7 MPa (the minimum installation pressure) to 23.9 MPa at a rate of +1.12 MPa/min. The pressure increment was performed during this period of equilibrated temperature in order to minimise the stresses on the cermet and die that could otherwise be caused by thermal expansion. This pressure increase facilitated further mechanical densification of the cermet and full pressure was applied until the end of the sintering profile.

The SPS current pulses used throughout this experimentation had a length of 12 μs separated by a 2 μs intermission. Peak values for the drive potential and current were typically around 4 V and 1.3 kA respectively.

3. Results

A total of six tungsten–ceria cermets were successfully manufactured during this investigation. Upon removal of the cermets from the die, their mass and density was measured and recorded. These results were recorded in Table 1.

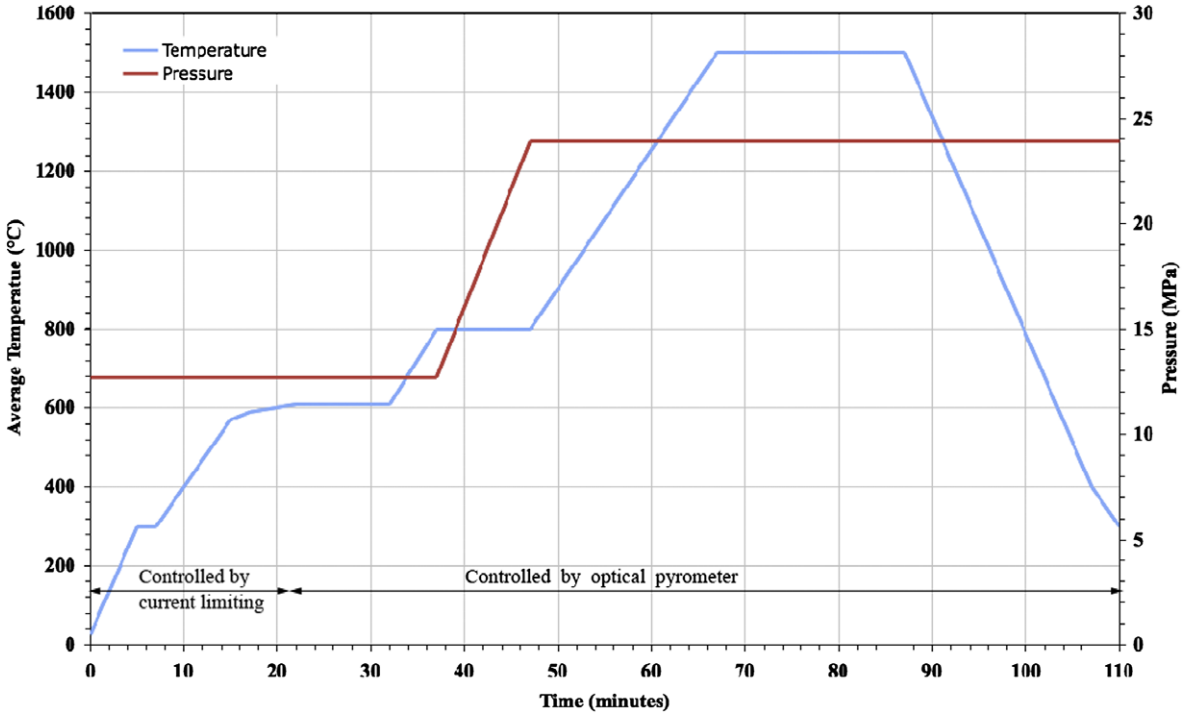

Fig. 4. Sintering temperature–pressure profile for W–CeO_2 cermets produced by SPS.

Table 1
Cermet density and mass results.

Volume tungsten (%)	Cermet serial number	Post sinter mass (g)	Measured density (g/cm^3)	Theoretical density (g/cm^3)	Average percent theoretical density (%)
50	ULCEW001	10.6	12.08	13.45	89.8
	ULCEW002	9.6	12.19		
	ULCEW003	11.5	11.96		
60	ULCEW004	9.3	13.81	14.61	94.2
	ULCEW005	10.7	13.78		
	ULCEW006	10.2	13.70		

In order to verify the elemental composition and hence mixture ratio of the cermets after sintering, the samples were cut and polished in preparation for examination by Scanning Electron Microscopy (SEM). The polishing process was achieved using a Struers TegraPol-21 polishing machine fitted with successfully fine grades of diamond polishing wheels. The early and intermediate stages of polishing were performed using 9 μm and 3 μm diamond suspensions respectively within a water based coolant/lubricant. The final stage of polishing was performed with a fine polishing cloth (Struers MD-CHEM) lubricated by a 0.04 μm colloidal silica suspension with a pH of 9.8 (Struers OP-S). The SEM system used was the Siron model (XLFEG/SFEG) SEM with Energy Dispersive X-Ray (EDX) capability and was manufactured by the FEI Company. Fig. 5 is an SEM image of cermet ULCEW004 indicating regions of CeO_2 and tungsten. Fig. 5 clearly shows the polycrystalline nature of the CeO_2 particles. It would appear that some cracking of the individual CeO_2 particles occurred during the application of high pressure to the mixture within the die. The voids created by this action were mostly filled by the 3–6 μm tungsten particles. A small volumetric fraction remained unfilled, accounting for some of the deficit in full densification of the cermets.

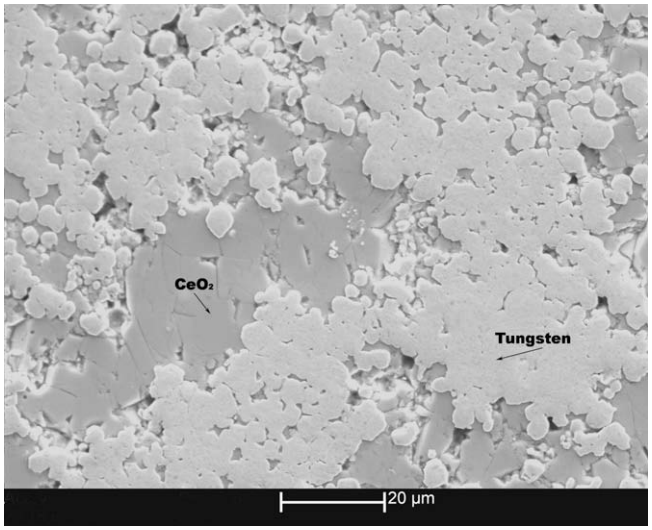

Fig. 5. Scanning Electron Microscope (SEM) image of a tungsten–ceria cermet cross section (serial ULCEW004). The cermet under examination was composed of 40% CeO_2 and 60% W by volume. This volumetric ratio is evident proportion of the cross sectional area covered by each material.

The density measurements were plotted against percentage of tungsten by volume so as to estimate a relationship between these two parameters (see Fig. 6). The results of Mataga [11] presented by German [7] indicate that for a heterogeneous mixture of 'active' and 'inert' sintering materials (where 'active' sintering materials are materials that sinter via neck formation such as the tungsten particles in the context of our research, and the 'inert' sintering materials are the ceramics that are to be encapsulated such as AmO_2), the relationship between the fractional density of sintered cermets and the percentage volumetric composition of 'active' sintering materials increases exponentially towards a maximum (~theoretical density) [7]. However, the data presented within this paper is only for the range 50–60%$_{Vol.}$ and lies in a portion of the Mataga curve [7,11] where the data can effectively be presented as linear although the data points may overall be part of an exponential curve. If the assumption is made that the data is part of an exponential relationship, it can be estimated that the density of a cermet expressed as a percentage of its theoretical density can be represented by the function $\rho(\%) \approx 70.6e^{0.0048[\%_{Vol.}W]}$ where $[\%_{Vol.}W]$ is the percentage of tungsten by volume that is mixed with the ceria for this specific combination of relative grain sizes over the range $50\% \leqslant [\%_{Vol.}W] \geqslant 60\%$. Based on the results of Mataga [11] and in conjunction with the data presented, it is predicted that it may be possible to achieve very high densities, close to theoretical density, with a greater volumetric ratio of W to CeO_2 when using the same feedstock morphology, although further experimental investigation is required to support this prediction and to verify the exponential relationship in greater resolution.

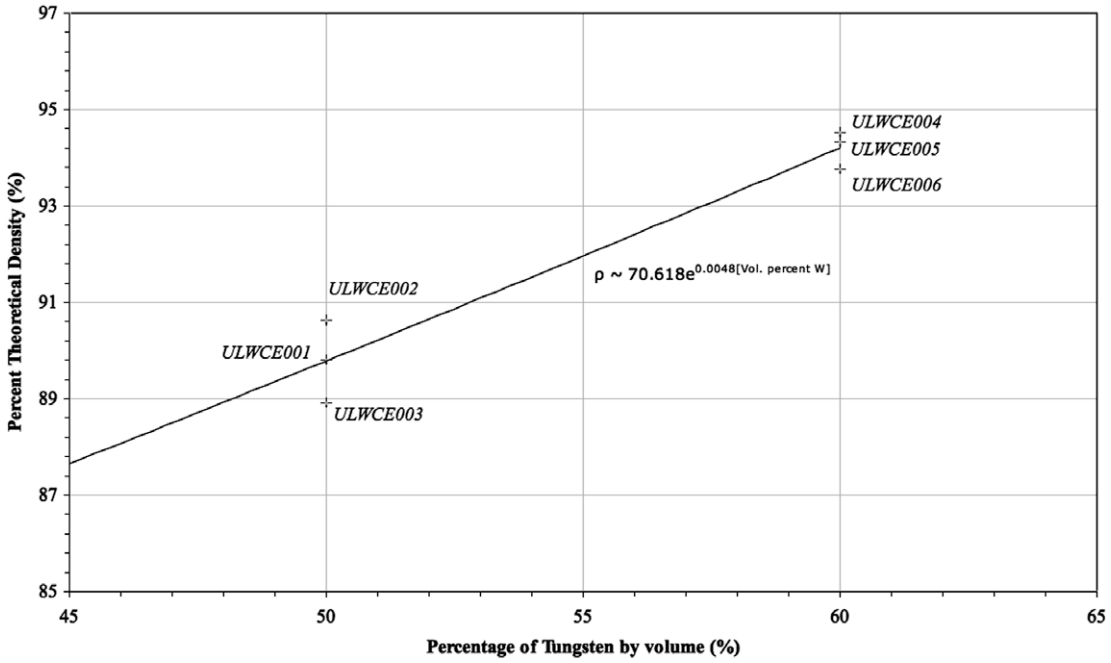

Fig. 6. Estimated relationship between the densities of product cermets expressed as a percentage of their theoretical density plotted as a function of the volumetric concentration of tungsten within the mixture over the range: $50\% \leqslant [\%_{Vol.}W] \geqslant 60\%$.

As is evident from the differences in cermet mass results (Table 1), it was expected that there would be some loss in mass primarily due to die leakage. Despite attempts to reduce the loss of material, the overall differences in the mass of each test product resulted in differing degrees of densification. Further analysis reveals that the die assemblies that lost the most mass of powdered material through leakage resulted in the highest recorded cermet densities. The variation in the densities of cermets produced from the same mixture ratios may be explained by assuming that the rate of densification per unit mass is a constant for any given die/furnace configuration. Thus, for a fixed sintering time period and die/furnace configuration, the average density of each sample is most fundamentally as a function of its initial mass or initial volume.

4. Conclusions and future work

The Spark Plasma Sintering process has been demonstrated to be compatible with the production of cermets consisting of simulated ceramic radioisotope materials and tungsten. Our work has shown that for applications where it may be necessary to control the porosity of cermets, the volumetric ratio of tungsten used in the cermets can be used to tune this porosity. Further investigation into the combined effect of volumetric ratios and grain size could reveal an accurate method for tuning the porosity of cermets and will be the focus of future work. Sub micrometer tungsten powder is of interest for use in cermet fabrication since it is believed that the smaller powder size will significantly enhance void filling between the ceramic grains and hence increase the density of the cermet for any given mixture.

Given that the leakage of gram quantities of powdered material from the dies was observed during pressing, consideration must be given to the minimization or elimination of furnace contamination if radioisotope materials are used. For this reason, operation of an SPS furnace for sintering radioisotope materials should be performed in an isolated environment such as in a glove box or hot cell. Although pre-pressing of the die assemblies throughout the tests described in this paper minimised material leakage in the furnace, the group will investigate the advantages of the use of binders and alternative die designs that will facilitate the SPS sintering process while maintaining an internal seal. Such die designs may eliminate the requirement of pre-pressing prior to the insertion of an assembled die into the furnace.

Further enhancement of densification could be achieved by the minimisation of shearing and cracking of the ceramic materials during the application of pressure. Future investigations will examine the production of, and the advantages of using spherical ceramic particles over granular ceramics. It is anticipated that spherical particles will be capable of resisting shear caused by the surrounding tungsten particles.

Overall, this work demonstrates the capability and suitability of the SPS process to the production of radioisotope encapsulates for nuclear fuels and other applications where the mechanical capture of radioisotope materials is required.

Acknowledgements

The Authors wish to thank the following people for their support through this research:

Douglas Burkes, Mark Henry, Stephen Johnson, Rory Kennedy, Kristi Martin, Harold McFarlane, James Werner and William Windes – Idaho National Laboratory.

Baden Favill – Space Research Centre, University of Leicester

Phil Stapleton – Department of Physics and Astronomy, University of Leicester

Tess Howell – Department of Materials Science and Engineering, University of Idaho

Daniel Osterberg – College of Engineering, Boise State University

The Engineering and Physical Sciences Research Council (EPSRC) for funding this research.

References

[1] R.C. O'Brien, R.M. Ambrosi, N.P. Bannister, S.D. Howe, H.V. Atkinson, J. Nucl. Mater. 377 (2008) 506.
[2] General Electric. 710 High-Temperature Gas Reactor Program Summary Report, Volume III, Fuel Element Development, General Electric, Pages 146, GEMP-600 (Vol. 3).
[3] X. Wang, Y. Xie, H. Guo, O. Van der Biest, J. Vleugels, Rare Metals 25 (2006) 246.
[4] H.V. Atkinson, S. Davies, Metall. Mater. Trans. A 31 (2000) 2981.
[5] A. Xu, A.A. Solomon. The effects of grain growth on the intergranular porosity distribution in hot pressed and swelled UO_2, in: Proceedings of Ceramic Microstructures '86, 28–31 July 1986, University of California, Plenum, Berkely, CA, 1986, ISBN: 0306426811.
[6] F.M.A. Carpay. The effect of pore drag on ceramic microstructures, in: Proceedings of Ceramic Microstructures '76, Westview, Boulder CO, 1977, p. 171, ISBN: 0891583076.
[7] R.M. German, Sintering Theory and Practice, John Wiley, New York, 1996, ISBN 0-471-05786-X.
[8] M. Rosinski, E. Fortuna, A. Michalski, Z. Pakiela, K.J. Kurzydlowski, Fus. Eng. Des. 82 (2007) 2621.
[9] J. Zhang, L. Wang, W. Jiang, L. Chen, Mater. Sci. Eng. A 487 (2008) 137.
[10] C.-C. Jia, H. Tang, X.-Z. Mei, F.-Z. Yin, X.-H. Qu, Mater. Lett. 59 (2005) 2566.
[11] P.A. Mataga, Retardation of sintering in heterogeneous powder compacts, in: C.A. Handwerker, J.E. Blendell, W.A. Kaysser (Eds.), Sintering of Advanced Ceramics, American Ceramic Society, Westerville, OH, 1990, ISBN 0944904203, p. 689.